

## RESEARCH LETTER

10.1002/2016GL070271

## Key Points:

- Volcanic vents <19 ka in the Somma-Vesuvius offshore near the coast
- Lava delta in the offshore formed between about 1000 and 1861 A.D.
- Submarine volcanism and lava entering the sea must be included in the Vesuvian area hazard evaluation

## Correspondence to:

V. Paoletti,  
paoletti@unina.it

## Citation:

Paoletti, V., S. Passaro, M. Fedi, C. Marino, S. Tamburrino, and G. Ventura (2016), Subcircular conduits and dikes offshore the Somma-Vesuvius volcano revealed by magnetic and seismic data, *Geophys. Res. Lett.*, 43, 9544–9551, doi:10.1002/2016GL070271.

Received 1 JUL 2016

Accepted 8 SEP 2016

Accepted article online 10 SEP 2016

Published online 23 SEP 2016

Corrected 17 JUN 2017

This article was corrected on 17 JUN 2017. See the end of the full text for details.

## Subcircular conduits and dikes offshore the Somma-Vesuvius volcano revealed by magnetic and seismic data

V. Paoletti<sup>1</sup>, S. Passaro<sup>2</sup>, M. Fedi<sup>1</sup>, C. Marino<sup>1</sup>, S. Tamburrino<sup>3</sup>, and G. Ventura<sup>2,4</sup>

<sup>1</sup>Dipartimento di Scienze della Terra, dell'Ambiente e delle Risorse, University Federico II, Naples, Italy, <sup>2</sup>IAMC-CNR Istituto per l'Ambiente Marino Costiero, Naples, Italy, <sup>3</sup>IAMC-CNR, UOS di Capo Granitola, Trapani, Italy, <sup>4</sup>INGV, Istituto Nazionale di Geofisica e Vulcanologia, Rome, Italy

**Abstract** We analyzed new magnetic, bathymetric, and seismic data acquired in the offshore sector of Somma-Vesuvius volcano (Italy). We detected a group of high-intensity, short wavelength magnetic anomalies corresponding to partly buried volcanic dome-like structures located by seismic data. The magnetic anomalies are aligned along a NW-SE strike that is the preferential orientation of an eruptive fracture of the pre-19 ka activity of Vesuvius. Four cones emplaced after the Last Glacial Maximum (19 ka), whereas a fifth one emplaced more recently suggesting a rejuvenation of the eruptive system offshore the volcano in historical times. We also identified a NE-SW elongated magnetic anomaly consistent with a dike-like body associated to an on-land tectonic structure that was active in recent times at Vesuvius. A delta-like area with diffuse low-intensity magnetic anomalies reflects the seaward fronts of lava flows that entered the sea mainly during the Middle Ages.

### 1. Introduction

Coastal volcanism is an open challenge in the field of risk evaluation due to the density of population living on coastal areas and the potential effects, e.g., tsunami, that may arise from volcanic events [Lipman and Moore, 1996; Keating and McGuire, 2000; Nemeth and Cronin, 2009]. Gulf of Naples (Italy) is an area potentially exposed to coastal volcanism due to the presence of the active volcanoes of Ischia, Campi Flegrei, and Somma-Vesuvius and to the large number of persons (about one million) living along the coast [Piochi et al., 2005]. Somma-Vesuvius last erupted in 1944, and its eruptive history includes highly explosive, mixed, and effusive events [e.g., Santacroce, 1987; Cioni et al., 2008]. The volcano is monitored by Osservatorio Vesuviano-INGV (<http://www.ov.ingv.it/ov/en/vesuvio/attivita-recente.html>), but its submarine, coastal sectors are still poorly known. Here we present and analyze high-resolution magnetic data, Sparker and Chirp monochannel seismic profiles, and bathymetric data acquired in the southwestern offshore of Somma-Vesuvius (Figure 1). The surveys were carried out with the aim to obtain key information on the submerged structure of the volcano and on its possible connections with known on-land volcanological and structural features.

### 2. Volcanological Setting

Gulf of Naples (Figure 1) is affected by prevailing NW-SE and NE-SW striking normal faults [Bruno et al., 2003]. Intense volcanism has characterized this area since middle Pleistocene. The onset of widespread volcanic activity and the consequent formation of a number of volcanic centers in the coastal zone of Campania (Campi Flegrei and Somma-Vesuvius) played a major role in shaping the morphology of the coastal landscape and continental shelf [Sacchi et al., 2005]. The eruption of the Campania Ignimbrite (39 ka) [De Vivo et al., 2001] in Campi Flegrei, and the plinian and subplinian deposits from Somma-Vesuvius flooded the whole coastal plain and the continental shelf of the Gulf of Naples [Fusi et al., 1991; Sacchi et al., 2005]. Somma-Vesuvius, which is located east of Campi Flegrei, resulted from the superimposition of two edifices: the older Mount Somma caldera (about 18 ka) [Santacroce, 1987] and the younger Vesuvius cone (1281 m above sea level (asl)), which formed between the 1631 A.D. and 1944 A.D. inside the Mount Somma caldera.

The eruptive history of the volcano has been characterized by plinian and subplinian eruptions occurred between 18 ka and 1631 A.D., and by lower energy explosive and effusive events, the last of which occurred in 1944 A.D. [Cioni et al., 2008]. Several lava flows of the Middle Age and historical times mantled the southwestern slope of the volcano. In particular, the lava flows erupted around the tenth century and those of the

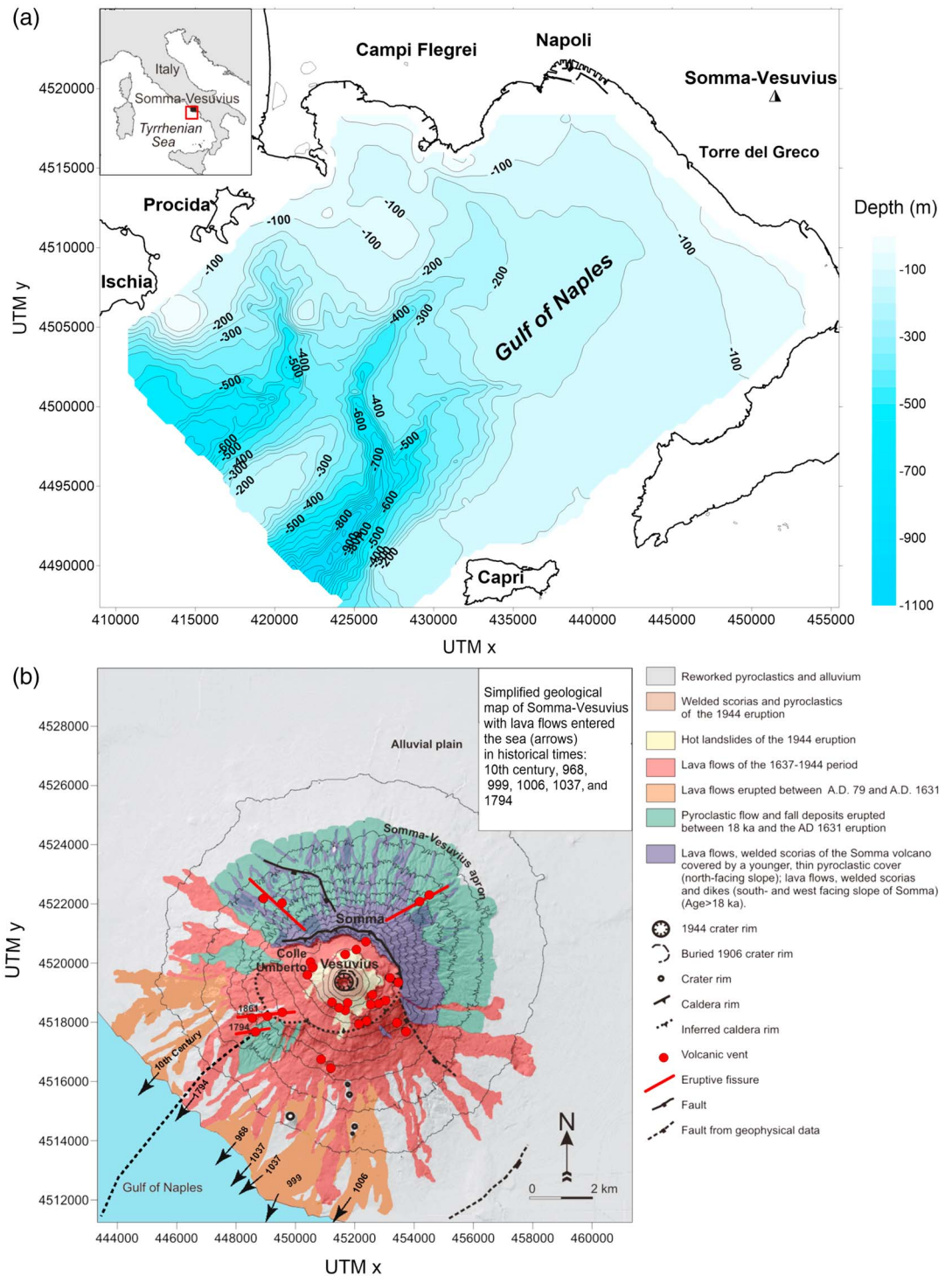


**Figure 1.** (a) Location map and bathymetry of the Gulf of Naples. Data are from *Secomandi et al.* [2003]. (b) Simplified geological map of the Somma-Vesuvius volcano with age of the lava flows which entered the sea. Data are from *Santacroce* [1987], *Bianco et al.* [1998], *Santacroce et al.* [2003], and *Principe et al.* [2004].

fissural, 1794 eruption, entered the sea [*Principe et al.*, 2004]. The structural setting of the volcano is characterized by dikes, emplaced by fissural eruptions, that follow a radial arrangement with NW-SE and NE-SW prevailing trends. These preferential patterns of dikes suggest a possible structural control played by regional faults [*Milia et al.*, 2012]. Seismic reflection data in Gulf of Naples [e.g., *Bruno et al.*, 2003; *Sacchi*

*et al.*, 2005] show faults that cut Pleistocene sediments with a prevailing NE-SW strike. In particular, a NE-SW fault (i.e., the Vesuvian fault) [Bruno *et al.*, 1998] and its presumable landward continuation may have played a major role in magma rising because of eruptive fissures with NE-SW strike were active in the pre-19 ka and historical times.

An important NE-SW lineament cutting the Somma-Vesuvius structure, recognized in literature as a strike slip fault and only partially identified in seismic researches, was clearly identified by Florio *et al.* [1999], thanks to a boundary analysis of gravity data. A 3-D density model [Cella *et al.*, 2007], reconstructing the top of the carbonate basement from inversion of gravity data, highlighted that compact material surrounds the central axis of the volcanic structure (as also sampled in the Trecase 1 well) [Bocchini *et al.*, 2001]. The density model also showed a weakness of the southwestern side of the volcano as one of the effects of the subsidence of the Mesozoic carbonate basement along NW faults toward the Gulf of Naples.

A high-resolution airborne magnetic survey carried out in 1999 in the Somma-Vesuvius area recognized several sources both onshore and offshore, interpreted as small local vents [Paoletti *et al.*, 2005a, 2005b]. However, the geometry, age, and structural significance of these vents were not characterized. Recently, vents of fluids were discovered and sampled also in the marine sector [Passaro *et al.*, 2014], where they are made up by volcanic CO<sub>2</sub> and mainly linked to the interaction between volcanism, bathymetry and regional faults [Passaro *et al.*, 2016a], or related to seafloor doming [Passaro *et al.*, 2016b] triggered by buried pockets of gas overpressure [Ventura *et al.*, 2016]. Previous marine geophysical studies (magnetometric and seismic) investigated the offshore of Somma-Vesuvius [Aiello *et al.*, 2001; Secomandi *et al.*, 2003]. These studies identified some dome-like structures located about 4 km offshore Torre del Greco and interpreted as cryptodomes and pit craters [Milia *et al.*, 2012].

### 3. Data and Methods

New magnetic, bathymetric, and seismic data were acquired during the “SAFE\_2014” survey carried out by Institute for the Coastal Marine Environment of National Research Council on board the R/V *Urania* on August 2014. About 600 km of magnetic and seismic profiles were collected offshore the Somma-Vesuvius volcano. More specifically, we acquired 40 profiles spaced 200 m and trending NW-SE (Figure 2a). Navigation was tracked thanks to the PDS2000 software (Tales©Inc.) equipped with a Differential Global Positioning System with instantaneous differential correction; this ensured a submetric precision for positioning. The positioning string was real-time sent to the acquisition equipment, properly corrected for its specific offset. The data were then georeferenced and plotted using the WGS84-UTM (Zone 33) projection system.

#### 3.1. Magnetic Data Layout and Processing

Magnetometric acquisition was made by the EG&G Geometrics caesium magnetometer G882 with an instrumental resolution of 0.01 nT. The magnetometer was towed astern with a constant 280 m layback from the ship and 12–15 m below sea level (bsl). Sampling time was 1 s. The processing of magnetic data included the following steps: (i) removal of spikes and gaps in the data carried out by manual editing; (ii) Earth's magnetic field diurnal variation corrections. The removal of the diurnal component was performed by selecting as base station of the geomagnetic observatory of Duronia, Italy (41°39'N–14°28'E); (iii) removal of the IGRF (International Geomagnetic Reference Field) performed employing the IGRF 2012 (<http://www.ngdc.noaa.gov/geomag-web/>); (iv) decorrugation, a directional filter allowing the removal of the directional anomalies along the navigation lines, based on the *Discrete Wavelet Transform* [Fedi and Florio, 2003; Paoletti *et al.*, 2007]. The map of the Somma-Vesuvius offshore obtained after data processing and data interpolation with the minimum curvature algorithm and a grid-node spacing of 100 m is shown in Figure 2a. The map highlights the presence of several anomalies extending about 2.5 km offshore from Torre del Greco and 10 km along the coast.

#### 3.2. Bathymetric, Seismic Data Layout, and Processing

The bathymetric survey was carried out by using a Simrad EM 710 multibeam equipment (Kongsberg©Inc.). The echosounder is characterized by a 70–100 kHz acoustic source frequency, 400 soundings per swath, and 140° of pulse width and allow data acquisition until 1200 m depth (2000 m in cold waters with low salinity). Sound velocity profiles were recorded and applied in real time during the acquisition, every 12–14 h. Multibeam swath bathymetry data have been processed according the International Hydrographic

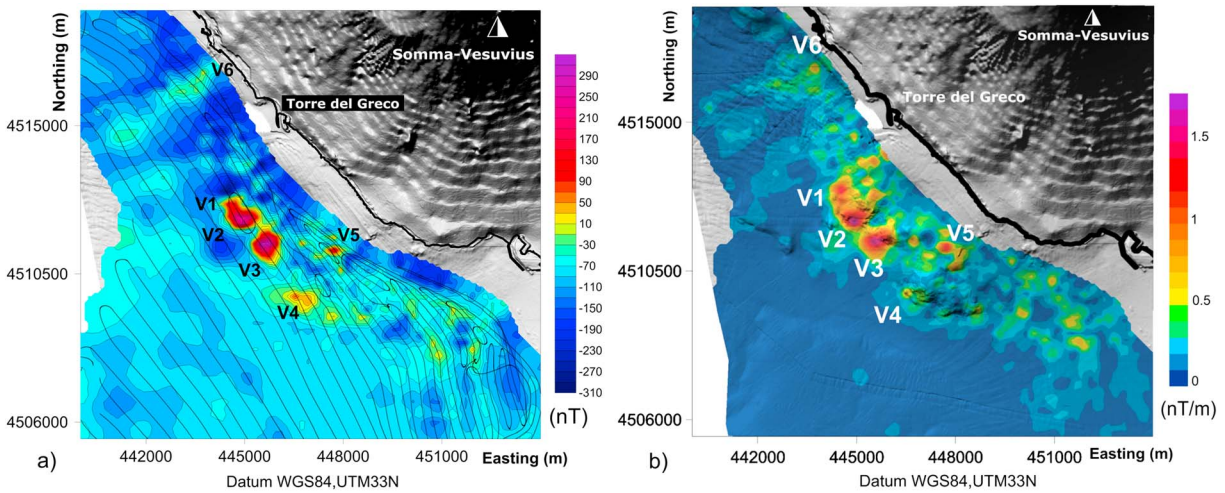


**Figure 2.** (a) Magnetic survey lines acquired in the Vesuvian offshore during the oceanographic survey SAFE\_2014 overlaid to the high-resolution magnetic map of the area. (b) Total magnetic gradient map overlaid to the high-resolution bathymetric data of the area.

Organization standards [International Hydrographic Organization, 2008], with the removal of wrong measurements (despiking). The data were reorganized in a 10 × 10 m grid cell size matrix (DTM, Digital Terrain Model). Chirp data acquisition was carried out by using a 16 transducers hull-mounted CHIRP-II profiler (Benthos Datasonics@Inc.), with operating frequencies in the range 2–7 kHz (Figure 3a). During the acquisition, the pulse length was selected between 10 ms and 500 ms, while the trigger rate changed from 0.5 to 2 s, depending on the water depth. Data were collected with the SWANPRO software by Communication Technology. Additional sparker profiles (Figure 3a) were acquired with a 1.4 kJ multitip Geospark seismic source interfaced with a Geotrace software (Geo-Marine Survey System). This system is made up by a

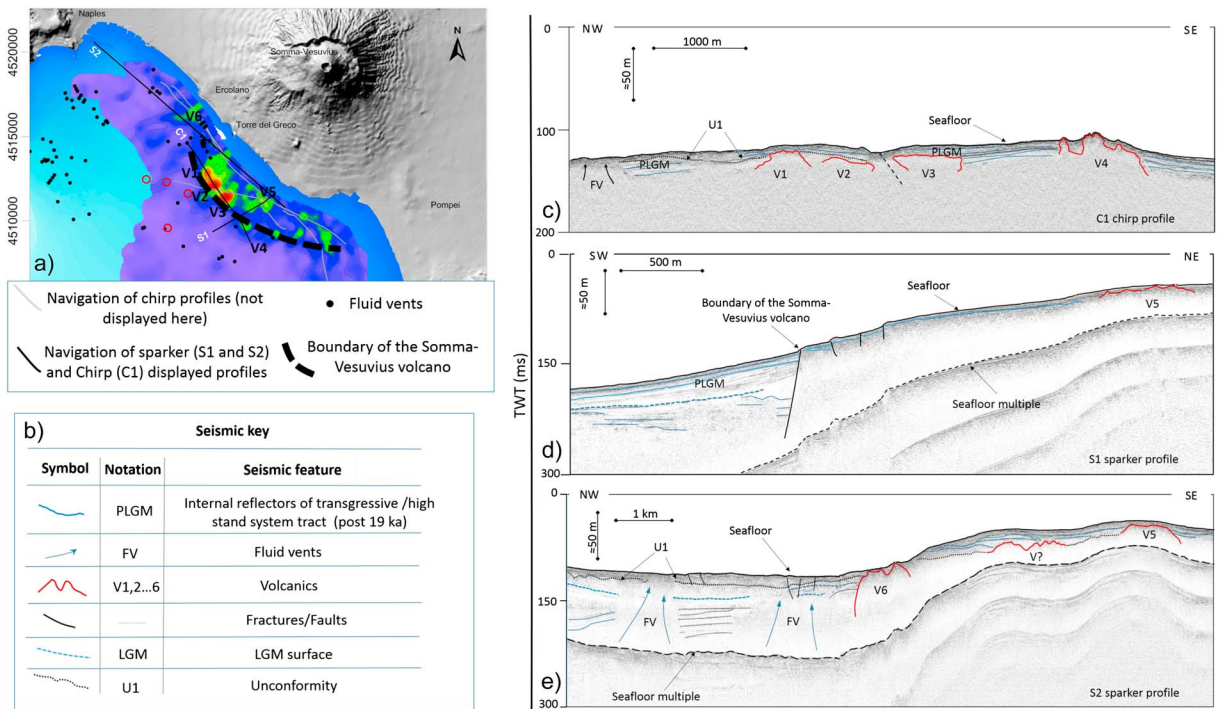


**Figure 3.** (a) Total magnetic gradient, gas emissions, and trace of the seismic profiles in the Vesuvius offshore; the “cryptodomes” structures of Milia et al. [2012] are reported as red circles. (b) Legend of symbol and notation used for the interpretation of seismic profiles; (c) C1 Chirp seismic profile; (d) S1 Sparker seismic profile; and (e) S2 Sparker seismic profile.

catamaran containing a 1–6.02 kHz seismic source that allows a penetration up to 400 ms below seabed and 30 cm of theoretical vertical resolution. The sparker profiles were acquired by using a 0.33 shot/s rate, and the vessel velocity was not exceeding 5.5 km/h. Both chirp and sparker seismic profiles were processed and presented by using the GeoSuite Allworks software with swell correction, muting of the water column, 2–6 kHz band-pass Infinite Impulse Response (IIR) filtering, and Automatic Gain Control.

#### 4. Results and Discussion

Magnetic data were used to compute a map of the total gradient (Figure 2b), which is only slightly dependent on the direction of the total magnetization vector [e.g., Nabighian *et al.*, 2005]. The total magnetic gradient map of the Somma-Vesuvius offshore shows a NW-SE alignment of anomalies in the offshore of Torre del Greco with a delta-like overall shape that corresponds with seafloor morphology. Some of these anomalies (i.e., V1, V2, and V3 in Figures 2 and 3) were already known from previous studies [Secomandi *et al.*, 2003; Aiello *et al.*, 2001], whereas others (V4, V5, and V6) are here reported for the first time. In order to characterize the sources of these magnetic anomalies, we used the imaging method *Depth from Extreme Points* method (DEXP) [Fedi, 2007]. The advantages of this method are speed and stability due to the regular behavior of potential field data versus the altitude, allowing consistent and high-resolution results even when using high-order derivatives of the field [Fedi and Pilkington, 2012]. The differentiation was performed through the Integrated Second Vertical Derivative (ISVD) procedure [Fedi and Florio, 2001] for the vertical derivatives, in the space domain for the horizontal derivatives and through the Fourier transform for the upward continuation. DEXP consists of scaling the field according to a power law of the altitude; the source depth may be estimated at its extreme points. The scaling exponent depends on the order of the vertical derivative of the potential field and on the structural index,  $N$ , which is a source parameter linked to the source geometry; it may be estimated through the “Multiridge Euler Deconvolution” method [Fedi *et al.*, 2009; Paoletti *et al.*, 2013] or automatically [Abbas and Fedi, 2014]. We estimated a structural index  $N=2$ , which is suitable for a circular conduit, for the V1, V2, and V3 anomalies and the less intense V4 anomaly. Figure 4a shows the result of 3-D DEXP analysis on V1–V3, with the depth of the sources being represented by the maxima of the DEXP function. The depths of the studied structures below the seabed are 20 m for the source of the anomaly V1 (i.e., 120 m bsl), and 40 m (140 m bsl) for the V2 and V3 sources; the DEXP analysis on the V4 anomaly (not shown in this paper) highlights a depth corresponding to the seabed. Given the found value of the structural index, those depths refer to the top of the source [Cella and Fedi, 2012]. The overall, fan-shaped displacement of magnetic anomalies corresponds to a set of seafloor morphological features available in the DTM and related to the evolution of the W-SW sector of Somma-Vesuvius (Figure 2b). Morphology in this area is ruled by the interactions of gravity processes and lavas and/or pyroclastic flows reworked by the sea level fluctuations. The joined magnetics-DTM map reveals a local, systematic correlation between the V1, V2, V3, and V4 anomalies and the seafloor morphology (Figure 2b). Chirp and seismic profiles helped to define the stratigraphic setting of magnetic sources (Figures 3a and 3b). According to previous studies [e.g., Sacchi *et al.*, 2005; Milia *et al.*, 2012], the layered, soft-sediment coverage mainly identifies transgressive and/or high stand sediments of the system tract emplaced after the Last Glacial Maximum (LGM, occurred about 19 ka B.P.). Within the post-LGM (PLGM) layers, tephra (dark reflectors) or small intervals made up by products arising from landslides are present (Figures 3c–3e). Locally, the continuity of reflectors is interrupted by the presence of fluid vents (FV, Figures 3c and 3e) that are also detectable at the sea bottom (Figure 3a). The U1 unconformity can be detected in the upper part of the Somma-Vesuvius slope and may be either the result of subaerial erosion (e.g., due to incised valley) or of a diffuse failure (Figures 3d and 3e). If we hypothesize that U1 is linked to an incised valley, it should be older than the transgressive/high stand stratigraphic change in the system tract depositional regime. However, U1 is surely younger than LGM. Main bedrock contacts can be relatively dated by taking into account their location with respect to the PLGM layers and the U1 unconformity.

Bedrock acoustic facies show indented or sharp margins, thus allowing the distinction between volcanic (V) and sedimentary basement. Inside PLGM, four main volcanic bodies are visible in the C1 seismic profile (Figure 3a), showing upper edges that are consistent with magnetic boundaries inferred by the total gradient of magnetic data, i.e., the V1, V2, V3, and V4 anomalies. The depth to the top of those volcanic bodies (Figure 3a) matches with that highlighted by magnetic data analysis (Figure 4). A relative dating can be obtained by using U1 as a marker level. V4 and V6 seem to be the earliest volcanic features, given their

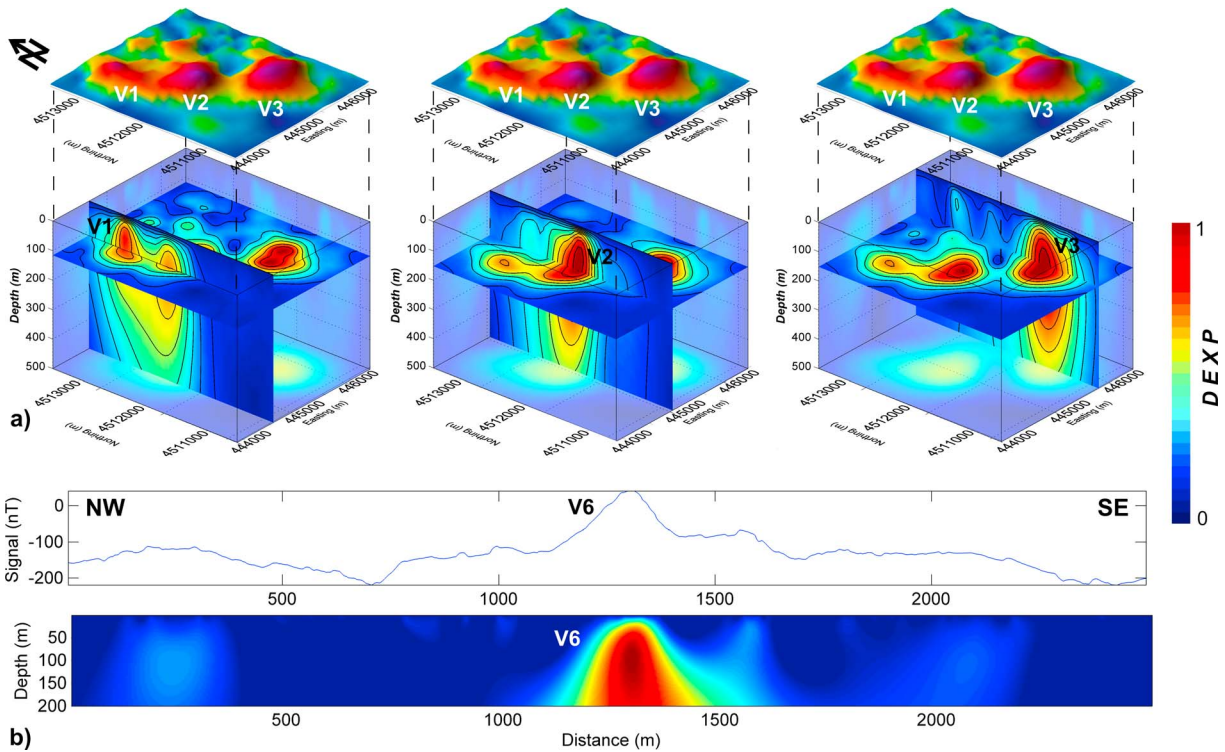


**Figure 4.** (a) 3-D depth analysis carried out through the DEXP method [Fedi, 2007] on anomalies V1, V2, and V3 in the Torre del Greco offshore. Upper plots show total magnetic gradient data (for colorbar and units please refer to Figure 2b). Lower plots show the outcome of the DEXP for the x coordinates 444600, 444900 and 445800, respectively. The resulting depths are referred to the sea level. (b) Two-dimensional depth analysis carried out through the DEXP method on the NE-SW magnetic lineament V6. Upper plot shows magnetic data. Lower plots show the outcome of the DEXP. For both the DEXP analyses in Figures 4a and 4b, normalized dimensionless units are used.

location in proximity of the actual bathymetry and the thin sediment coverage (Figures 3c and 3e). Main bedrock contacts located below PLGM show indented or sharp margins, thus allowing distinguishing the volcanic (V) rocks from the sedimentary succession. Four main volcanic bodies (V1–V4) are visible in the C1 seismic profile (Figure 3c), showing edges that perfectly match with the sources inferred by the total magnetic gradient map. These structures have widths in the range 700–1000 m (Figure 3c). Their shape is that of subcircular cones or domes, a result well matching the conduit-like geometries obtained from the imaging of the magnetic data. Therefore, the magnetic anomalies V1–V3 possibly represent the crystallized, shallowest plumbing system (conduit) of these volcanic cones. As concerns the age of these structures, the seismic profiles show that the V1 to V3 volcanics are covered by the PLGM sediments and draped following an onlap-type contact by the U1 unconformity. Therefore, their age is post-19 ka. The less intense magnetic anomaly V4 corresponds to an articulated morphostructure in the seismic profiles (V4 in Figure 3c). This structure is not covered by the PLGM or actual sediments, and it is surrounded by faults possibly formed during the emplacement of V4. Therefore, the formation of V4 is post-U1. We conclude that this last volcanic structure, whose seismic features are consistent with a neck-like body, is younger than the V1–V3 ones.

Regarding the V5 source, we estimated a structural index suitable for a circular conduit. Its depth is 70 m from the seabed, i.e., 110 below the sea level, as inferred from the results of the DEXP analysis (not shown in this paper). In the Sparker seismic profile S2, the body possibly corresponding to the V5 source is characterized by a semitransparent seismic facies that lies below poorly stratified sediments disturbed by chaotic horizons. Therefore, this profile does not allow us to better constrain the morphology of the V5 source. On the seismic profile, the V5 top is 1–5 m below the seabed (Figures 3d and 3e). Taking into account the previously discussed stratigraphic relations among the sediments and the V1 to V4 sources, which also hold for V5, we suggest that the V5 body is younger than 19 ka as well.

The 2-D DEXP analysis on the V6 NE-SW striking magnetic lineament, along a NW-SE profile, shows that the top of the source is located 50 m below the seabed (i.e., 100 m bsl) (Figure 4b). For this source, we estimated

through the *Multiridge Euler Deconvolution* method a structural index  $N = 1$ , corresponding to a dike-like geometry. V6 is located in correspondence with a regional structure (Torre del Greco fault) [Finetti and Morelli, 1974] interpreted as preferential path of magma ascent in the pre-19 ka and post-1631 A.D. periods of activity, in particular during the 1794 and 1861 A.D. eruptions (see Figure 1) [Bianco *et al.*, 1998; Principe *et al.*, 2004]. Therefore, taking into account the value of the structural index and the NE-SW elongation of the magnetic anomaly (Figure 2), we conclude that V6 represents a NE-SW striking dike possibly emplaced within this tectonic structure of regional significance. On the seismic profile, the V6 top is 1–5 m below the present-day seabed (Figure 3d). The lack of seismic profiles in this area does not permit to constrain the age of V6. The differences in the depths inferred by the magnetic and seismic analyses on V5 and V6 may be due to a lack of magnetization of the shallowest section of those bodies.

As concerns the offshore “cryptodomes” detected at a distance of 4 km from the coast by Milia *et al.* [2012], our data do not show magnetic anomalies located above them (Figure 3a). Therefore, their volcanic or intrusive nature is questionable. The semitransparent seismic facies of the structures inferred by Milia *et al.* [2012] well characterizes the subseabed CO<sub>2</sub> degassing conduits of Gulf of Naples [Passaro *et al.*, 2016a, 2016b]. Thus, we suggest that these structures may represent degassing conduits. Finally, our data show that the high-intensity magnetic sources studied here are located in an area of widespread, diffuse, and low-extension anomalies forming a delta-like magnetic sector in front of the southwestern flanks of Somma-Vesuvius (Figures 2b and 3a). The pattern of the magnetic anomalies shows a radial displacement with respect to the main Somma-Vesuvius edifice. This magnetic pattern coincides with a stratigraphic boundary that separates an area with a larger sedimentary coverage (seaward) from a second one (landward) characterized by a thinner coverage of sediments lying over the volcanic bedrock (Figure 3d). Thus, the sharp stratigraphic and magnetic boundary separates the magnetic fan-shaped area from the distal sector of the shelf (Figures 3a–3d). This morphologic, stratigraphic, and magnetic boundary probably marks the west-southwest outer limit of the Somma-Vesuvius volcano. Because several Medieval lava flows entered the sea (Figure 1) [Principe *et al.*, 2004], we may suppose that the delta-like magnetic coastal sector of the volcano reflects the offshore propagation of these historical lavas.

## 5. Conclusive Remarks

The high-intensity magnetic anomalies, NW-SE aligned, recognized in the Somma-Vesuvius offshore represent volcanic dome-like structures related to the post-19 ka activity. This NW-SE strike follows that of the major faults affecting Gulf of Naples as well as that of the major eruptive fissure affecting the northwestern flank of the Somma-Vesuvius volcanic complex. Therefore, we conclude that the detected volcanic vents emplaced along a fracture having regional significance. A neck-like structure younger than 19 ka has been also detected south of the above-described cones suggesting a period of rejuvenation in the offshore sector of the Somma-Vesuvius volcano. A lower intensity NE-SW trending magnetic anomaly localized in correspondence of the Torre del Greco offshore may represent a dike intruded within a structurally weak zone of the Somma-Vesuvius volcano. Since the detected submerged neck-like structure emplaced during the more recent Vesuvius period, the hazard related to possible, future submarine activity should be included in the hazard evaluation programs. Finally, we detect morphologies consistent with submerged fronts of lava flows mainly erupted in Medieval times. Therefore, the hazard related to lava flows entering the sea should be taken into account for a correct planning of the expected eruptive scenarios.

### Acknowledgments

We thank Roman Pasteka and Claudia Principe for the perceptive review of the manuscript. This research has been supported by CNR-IAMC and University Federico II.

### References

- Abbas, M. A., and M. Fedi (2014), Automatic DEXP imaging of potential fields independent of the structural index, *Geophys. J. Int.*, *199*(3), 1625–1632, doi:10.1002/2016GL070271/pdf.
- Aiello, G., F. Budillon, G. Cristofalo, B. D'Argenio, G. de Alteriis, M. De Lauro, L. Ferraro, E. Marsella, N. Pelosi, and R. Tonielli (2001), Marine geology and morphobathymetry in the Gulf of Naples (south-eastern Tyrrhenian Sea, Italy), in *Mediterranean Ecosystems: Structures and Processes*, edited by E. M. Farina, L. Guglielmo, and G. Spezie, pp. 1–8, Springer, Berlin.
- Bianco, F., M. Castellano, G. Milano, G. Ventura, and G. Vilardo (1998), The Somma-Vesuvius stress field induced by regional tectonics: Evidences from seismological and mesostructural data, *J. Volcanol. Geotherm. Res.*, *82*, 199–218.
- Bocchini, D., C. Principe, D. Castratori, M. A. Laurenzi, and L. Gorla (2001), Quaternary evolution of the southern sector of the Campanian Plain and early Somma-Vesuvius activity: Insights from the Trecase 1 well, *Mineral. Petrol.*, *73*, 76–91.
- Bruno, P. P., G. Cippitelli, and A. Rapolla (1998), Seismic study of the Mesozoic carbonate basement around Mt. Somma-Vesuvius volcanic complex (Italy), *J. Volcanol. Geotherm. Res.*, *84*, 311–322.

- Bruno, P. P., A. Rapolla, and V. Di Fiore (2003), Structural settings of the Gulf of Naples (Italy) by seismic reflection data: Implications for Campanian volcanism, *Tectonophysics*, 372, 193–213.
- Cella, F., and M. Fedi (2012), Inversion of potential field data using the structural index as weighting function rate decay, *Geophys. Prospect.*, 60, 313–336, doi:10.1111/j.1365-2478.2011.00974.x.
- Cella, F., M. Fedi, G. Florio, M. Grimaldi, and A. Rapolla (2007), Shallow structure of the Somma-Vesuvius volcano from 3D inversion of gravity data, *J. Volcanol. Geotherm. Res.*, 161(4), 303–317, doi:10.1002/2016GL070271/pdf.
- Cioni, R., A. Bertagnini, R. Santacroce, and D. Andronico (2008), Explosive activity and eruption scenarios at Somma-Vesuvius (Italy): Towards a new classification scheme, *J. Volcanol. Geotherm. Res.*, 178(3), 331–346, doi:10.1007/s00445-010-0379-2.
- De Vivo, B., G. Rolandi, P. B. Gans, A. Calvert, W. A. Bohrson, F. J. Spera, and H. E. Belkin (2001), New constraints on the pyro-clastic eruptive history of the Campanian Volcanic Plain (Italy), *Min. Pet.*, 73, 47–65.
- Fedi, M. (2007), DEXP: A fast method to determine the depth and the structural index of potential fields sources, *Geophysics*, 72(1), 11–111.
- Fedi, M., and G. Florio (2001), Detection of potential fields source boundaries by enhanced horizontal derivative method, *Geophys. Prospect.*, 49, 40–58.
- Fedi, M., and G. Florio (2003), Decorrugation and removal of directional trends of magnetic fields by the wavelet transform: Application to archaeological areas, *Geophys. Prospect.*, 51(4), 261–272.
- Fedi, M., and M. Pilkington (2012), Understanding imaging methods for potential field data, *Geophysics*, 77(1), G13–G24.
- Fedi, M., G. Florio, and T. Quarta (2009), Multiridge analysis of potential fields: Geometrical method and reduced Euler deconvolution, *Geophysics*, 74, L53–L65.
- Finetti, I., and C. Morelli (1974), Esplorazione sismica a riflessione dei Golfi di Napoli e Pozzuoli, *Boll. Geofis. Teor. Appl.*, 62–63, 175–221.
- Florio, G., M. Fedi, F. Cella, and A. Rapolla (1999), The Campanian Plain and Phlegrean Fields: Structural setting from potential field data, *J. Volcanol. Geotherm. Res.*, 91(2–4), 361–379.
- Fusi, N., L. Mirabile, A. Camerlenghi, and G. Ranieri (1991), Marine geophysical survey of the Gulf of Naples (Italy): Relationships between submarine volcanic activity and sedimentation, *Mem. Soc. Geol. Ital.*, 47, 95–114.
- International Hydrographic Organization (2008), *International Hydrographic Organization Standards for Hydrographic Surveys, Spec. Publ.*, vol. 44, pp. 28, International Hydrographic Bureau, Monaco.
- Keating, B., and W. McGuire (2000), Island edifice failures and associated tsunami hazards, *Pure Appl. Geophys.*, 157(6–8), 899–955.
- Lipman, P., and J. Moore (1996), Mauna Loa lava accumulation rates at the Hilo drill site: Formation of lava deltas during a period of declining overall volcanic growth, *J. Geophys. Res.*, 101(B5), 11,631–11,641, doi:10.1029/95JB03214.
- Milia, A., M. M. Torrente, and F. Bellucci (2012), A possible link between faulting, cryptodomes and lateral collapses at Vesuvius Volcano (Italy), *Global Planet. Change*, 90–91, 121–134.
- Nabighian, M. N., V. J. S. Grauch, R. O. Hansen, T. R. LaFehr, Y. Li, J. W. Peirce, J. D. Phillips, and M. E. Ruder (2005), The historical development of the magnetic method in exploration, *Geophysics*, 70, 33ND–61ND, doi:10.1190/1.2133784.
- Nemeth, K., and S. Cronin (2009), Phreatomagmatic volcanic hazards where rift systems meet the sea, a study from Ambae Island, Vanuatu, *J. Volcanol. Geotherm. Res.*, 180(2–4), 246–258.
- Paoletti, V., R. Supper, M. Chiappini, M. Fedi, G. Florio, and A. Rapolla (2005a), Aeromagnetic survey of the Somma-Vesuvius volcanic area, *Ann. Geophys.*, 48, 199–213, doi:10.1007/s10712-015-9352-0.
- Paoletti, V., M. Secomandi, G. Florio, M. Fedi, and A. Rapolla (2005b), The integration of remote sensing magnetic data in the Neapolitan volcanic district, *Geosphere*, 1, 85–96, doi:10.1002/2016GL070271/pdf.
- Paoletti, V., M. Fedi, G. Florio, and A. Rapolla (2007), A localized cultural de-noising of high-resolution aeromagnetic data, *Geophys. Prospect.*, 55, 412–432.
- Paoletti, V., S. Ialongo, G. Florio, M. Fedi, and F. Cella (2013), Self-constrained inversion of potential fields, *Geophys. J. Int.*, 195(2), 854–869.
- Passaro, S., et al. (2014), First hydroacoustic evidence of marine, active fluid vents in the Naples Gulf continental shelf (Southern Italy), *J. Volcanol. Geotherm. Res.*, 285, 29–35.
- Passaro, S., S. Tamburrino, M. Vallefucio, S. Gherardi, M. Sacchi, and G. Ventura (2016a), High-resolution morpho-bathymetry of the Gulf of Naples, Eastern Tyrrhenian Sea, *J. Maps*, doi:10.1080/17445647.2016.1191385.
- Passaro, S., S. Tamburrino, M. Vallefucio, F. Tassi, O. Vaselli, L. Giannini, G. Chiodini, S. Caliro, S. M. Sacchi, and G. Ventura (2016b), Seafloor doming driven by degassing processes unveils sprouting volcanism in coastal areas, *Sci. Rep.*, 6, 22,448, doi:10.1038/srep22448.
- Piochi, M., P. P. Bruno, and G. De Astis (2005), Relative roles of rifting tectonics and magma ascent processes: Inferences from geophysical, structural, volcanological, and geochemical data for the Neapolitan volcanic region (southern Italy), *Geochem. Geophys. Geosyst.*, 6, Q07005, doi:10.1029/2004GC000885.
- Principe, C., J.-C. Tanguy, S. Arrighi, A. Paiotti, M. LeGoff, and U. Zoppi (2004), Chronology of Vesuvius' activity from A.D. 79 to 1631 based on archeomagnetism of lavas and historical sources, *Bull. Volcanol.*, 66, 703–724.
- Sacchi, M., D. Insinga, A. Milia, F. Molisso, A. Raspini, M. M. Torrente, and A. Conforti (2005), Stratigraphic signature of the Vesuvius 79 AD event off the Sarno prodelta system, Naples Bay, *Mar. Geol.*, 222–223, 443–469.
- Santacroce, R. (1987), *Somma-Vesuvius, Quaderni de La Ricerca Scientifica*, vol. 17, pp. 251, Cons. Naz. delle Ric., Rome.
- Santacroce, R., A. Sbrana, R. Sulpizio, and G. Zanchetta (2003), Carta geologica del Somma-Vesuvio, scale 1:15.000, S.EL.CA., Florence, Italy (in Italian).
- Secomandi, M., V. Paoletti, V. G. Aiello, M. Fedi, E. Marsella, S. Ruggieri, B. D'Argenio, and A. Rapolla (2003), Analysis of the magnetic anomaly field of the volcanic district of the Gulf of Naples, Italy, *Mar. Geophys. Res.*, 24, 207–221.
- Ventura, G., S. Passaro, S. Tamburrino, M. Vallefucio, and M. Sacchi (2016), A model-estimation of gas overpressure in gas saturated layers in a volcanic setting: A case study from the Banco della Montagna (Naples Bay, Italy). *Proceedings of the 1st IMEKO TC-4 International Workshop on Metrology for Geotechnics*, March 17–18, 2016, Benevento, Italy, 313–317.

## Erratum

In the originally published version of this article, the Abstract incorrectly referred to “three cones emplaced before the Last Glacial Maximum, [and] a fourth one emplaced after 19 ka.” The sentence has been corrected to refer to “four cones emplaced after the Last Glacial Maximum (19 ka), [and] a fifth one

emplaced more recently," as also clearly stated in the Conclusions. On page 3, we describe the structural setting of Somma-Vesuvius and refer to the "pre-18 ka" activity. This has been corrected to "pre-19 ka," here and also on page 7, third line. The confusion originated from the fact that the Last Glacial Maximum is dated 18 ka by some authors in the literature and 19 ka by other authors. On page 3, section 3.1, we describe the used instruments and we refer to a "proton magnetometer." This has been corrected to "caesium magnetometer." Figure 3 has been slightly changed by correcting the labels showing the directions of the C1 and S1 profiles (plots c and d). On page 6, second paragraph, third line, "P2" has been corrected to "S2." The present version may be considered the authoritative version of record.